

Article

Energy Consumption Comparison of a Single Variable-Speed Pump and a System of Two Pumps: Variable-Speed and Fixed-Speed

Safarbek Oshurbekov ¹, Vadim Kazakbaev ¹, Vladimir Prakht ^{1,*}, Vladimir Dmitrievskii ¹
and Levon Gevorgov ²

¹ Department of Electrical Engineering, Ural Federal University, 620002 Yekaterinburg, Russia; safarbek.oshurbekov@urfu.ru (S.O.); vadim.kazakbaev@urfu.ru (V.K.); vladimir.dmitrievsky@urfu.ru (V.D.)

² Faculty of Electrical Engineering, University of West Bohemia, 301 00 Pilsen, Czech Republic; levon@rice.zcu.cz

* Correspondence: va.prakht@urfu.ru; Tel.: +7-343-375-45-07

Received: 12 November 2020; Accepted: 7 December 2020; Published: 9 December 2020



Featured Application: The presented results can be used to assess the energy-saving potential of various topologies of multi-pump pumping stations.

Abstract: The energy efficiency of a multi-pump system consisting of two low-power (0.75 kW) pumps operating in parallel mode and a single-pump mechanism (1.5 kW) is compared in this study. For this purpose, mathematical models, experimental data, and data retrieved from the manuals provided by the pump manufacturers are used. The single-pump system is fed by a single variable speed drive. A multi-pump system running in parallel mode consists of two pumps. One of them is driven by an induction motor connected directly to the electrical grid and equipped with a throttle. Another pump is actuated by an induction motor fed by a variable speed drive. The flowrate of the liquid in the multi-pump is controlled with the help of speed variation and throttling. In the case of the single-pump system the conventional speed control method is applied during the analysis. For both pump system topologies, the daily and annual energy consumption is obtained. As a result of conducted calculations, it was shown that the multi-pump provides 29.8% savings in comparison to the single-pump system in the case of a typical flowrate profile.

Keywords: centrifugal pump; energy efficiency; induction motor; throttling control; variable speed control

1. Introduction

Pumping systems are among the main electrical energy consumers in industry and household applications. These systems account for approximately 22% of the energy consumed by electrical motors [1]. The problem of the energy efficiency of pumping systems is topical among the researchers [2,3]. Although most of the pumping units are still using drives without variable speed control [3], in some countries almost 20–30% of pumping systems are already supplied with variable speed drives (VSDs), due to their high efficiency [4].

Often, instead of a high-power single pumping system, a multi-pump system with two or more pumps with a lower power is used [5–7]. This type of solution can provide cheap operation costs, easier maintenance, and a longer lifespan of a pumping unit. In addition, there is a possibility of flowrate control in a multi-pump system without a pressure drop and significant efficiency drop of pumping units. It is almost impossible to achieve by means of either throttling or speed control in a

single-pump pumping system [8]. Maintaining the pressure in the system at flowrate control is crucial in applications with high static pressure [6,7].

The possibility of energy loss reduction for the multi-pump system is achieved with the help of switching off some of the pumps at low flowrates, as well as by optimizing the operation of separate pumps, in the case where they are supplied with variable speed drives [6–8].

A wide variety of articles concern the energy efficiency issues of multi-pump systems. In [8] for example, the optimization of multi-pump system operation is considered in order to increase reliability and improve the efficiency of the system. The efficiency of the two systems is compared depending on the fluid flowrate. For pumps operating in parallel mode, the possibility of the optimal control strategy is studied with the help of a genetic algorithm. The obtained results show that the highest efficiency is achieved by ensuring the same flowrate of two pumps. This article also studies the comparison of a system consisting of two pumps with one frequency converter and the same system with two separate frequency converters for each pumping unit. It is shown that the latter system has better efficiency.

In [9], the solution for energy efficiency boosting in a multi-pump system with variable speed drives is proposed. The concept does not include any additional flow meters or measuring instruments for flow-head characteristics. An original strategy for multi-pump system control using throttling and speed control methods based on flow rate estimation is proposed.

In [10], an original algorithm is proposed for reliable prediction of the operation of parallel controlled pumps in the multi-pump system and the control of the number of working pumps that is optimal from the energy efficiency point of view for variable speed drives without throttling implementation.

In [11], the parallel operation of two pumps with the same parameters of the nominal pressure and different values of the nominal flow is investigated. It is shown that the overall efficiency of the system decreases with an increase in the ratio of the nominal flow rates for individual pumps. For comparison, 28 various combinations of pump system parameters were investigated.

In [12,13], the parallel operation of the multi-pump system consisting of four pumps is considered, where the flowrate is controlled by three different methods (throttling, bypass, and by the speed regulation). A genetic algorithm is used to find the proper energy-efficient management strategy.

In [14], a system with five parallel pumps is investigated. The power consumption is compared for different cases. For instance, when only one frequency converter is used and in the case of using five separate frequency converters for each particular pump. It is shown that in the case of application of variable speed drives for each pump instead of one variable speed drive leads to a reduction of power consumption from the grid by 2.5%.

In [15], the optimization of the energy consumption of three parallel pumps without rotational speed regulation is considered. In [16], the optimization of the energy consumption of a system of seven parallel pumps of various types, some of which are equipped with VSD, is considered. In [17], the energy consumption of three pumps is compared when varying the number of VSDs. In [18], the energy consumption of pumping systems employing 2–4 parallel pumps without rotational speed regulation is compared.

The analysis shows that the use of variable speed drives for each pump in a multi-pump system is generally the most energy-efficient solution. A large number of proposed various control strategies achieved by using different optimization methods demonstrate the complexity and necessity to take into account a large number of parameters when optimizing the energy consumption of a multi-pump system. A series of research works are devoted to comparing the energy consumption of various multi-pump systems [6,14–19]. One of the issues that is not sufficiently described in the literature is the strategy for an optimal number of running pump selections in a multi-pump system for specific applications. In the case of low-power pumping units, the preferred option between single-pump and multi-pump configurations may not be obvious.

In particular, despite a large amount of literature on the analysis of the energy efficiency of various schemes of multi-pump systems, the energy efficiency of a pump unit with a single pump equipped with a VSD and a system with two pumps only one of which is equipped with a VSD has not been

compared earlier. This case is of great practical importance since both considered configurations can be used in small pumping stations.

The pumping system with two motors and one frequency converter is a special case of multi-motor pumping stations with a single frequency converter (single-drive multi-pump systems) for fluid machinery applications. Such systems are widely used in the electric drive of pumping and compressor stations employing pump/compressor units of low rated power. This makes it possible to significantly reduce the capital costs of such pumping stations while providing the smooth regulation of the pressure/flow rate [20–22].

In order to compare the operation of pumps with the mentioned topology, this paper presents a quantitative assessment of the energy consumption of a system consisting of two parallel pumps (0.75 kW), in comparison with a system containing one single pump (1.5 kW) that is driven by a VSD. A single-pump system contains only one variable speed drive for the induction motor (IM). The multi-pump system with two pumps in parallel contains one induction motor, fed directly from the grid, and a second induction motor, fed by the frequency converter. An induction motor connected directly to the grid drives a pump with throttle control. Both pumping systems have the same fluid flowrate that is specific for open loop pumping systems.

With the help of the mathematical model, data from the catalogues provided by the manufacturer, and experimental data, the energy consumption of the two types of pump system topologies is compared. Since the cost of a variable frequency drive is a significant part of the total price of a low-power pump system, the case of parallel operation of two pumps using one VSD is considered. In this study, we examine the feasibility of using two parallel pumps in the multi-pump system instead of a single-pump system, mainly taking into account energy efficiency.

2. Structure of the Examined Pump Systems

The following structures of the pumping system are examined in the project:

- The pumping system with a single pump supplied with a VSD, the nominal power of 1500 W, and the nominal speed of 2900 rpm. Water supply is controlled by the speed control method;
- The multi-pump system with two parallel pumps, the nominal power of 750 W, and the nominal speed of 2900 rpm. The electric drive of the first pump is equipped with a VSD, and the second pump has an induction motor connected directly to a grid. The water supply is controlled by the VSD of the first pump and by throttling of the second pump.

The energy consumption of these pump systems is compared for an application when the water supply during the cycle corresponds to the dependence typical for open loop pump systems [23]. The dependence is shown in Figure 1. The period of the cycle equals 24 h.

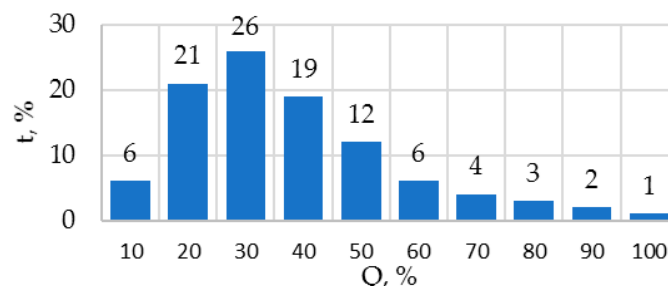


Figure 1. Flowrate-time dependence. Q , % is the percentage of the flow; t , % is the percentage of the time.

For a single-pump system, the pump Calpeda—B—40/12C/A (model 1) is chosen; the rated power is 1500 W [24]. For a multi-pump system, two pumps Calpeda—B—NM 32/12D (model 2) are chosen; the rated power is 750 W [24]. The rated rotational speed is 2900 rpm. Figure 2 represents

the Q - H characteristics and the dependencies of the shaft power on the flowrate for both pumps at the rated rotational speed. The two pumps under consideration have an identical no-load head of about 18 m but different maximum flow rates. The required maximum flow rate $Q_{100\%} = 24 \text{ m}^3/\text{h}$ can be provided by the single pump with the rated power of 1.5 kW (Figure 2a). When using the pumps with the rated power of 750 W, two such pumps are required to provide $Q_{100\%} = 24 \text{ m}^3/\text{h}$ (Figure 2b). The required mechanical power P_{mech} can be calculated as $H \cdot Q \cdot g \cdot \rho / \eta_{\text{pump}}$, where $g = 9.81 \text{ m/s}^2$ is the gravitational acceleration; $\rho = 1000 \text{ kg/m}^3$ is the water density; η_{pump} is the pump efficiency. However, for calculations in this study, P_{mech} is obtained from $P_{mech}(Q)$ dependences from the manufacturer’s catalogue (Figure 2c,d). The maximum required flowrates of both pumping systems were chosen to correspond to the flowrate of the pump Calpeda—B—40/12C/A at the best efficiency point (BEP) $Q_{100\%} = Q_{BEP1} = 24 \text{ m}^3/\text{h}$ (Figure 2e).

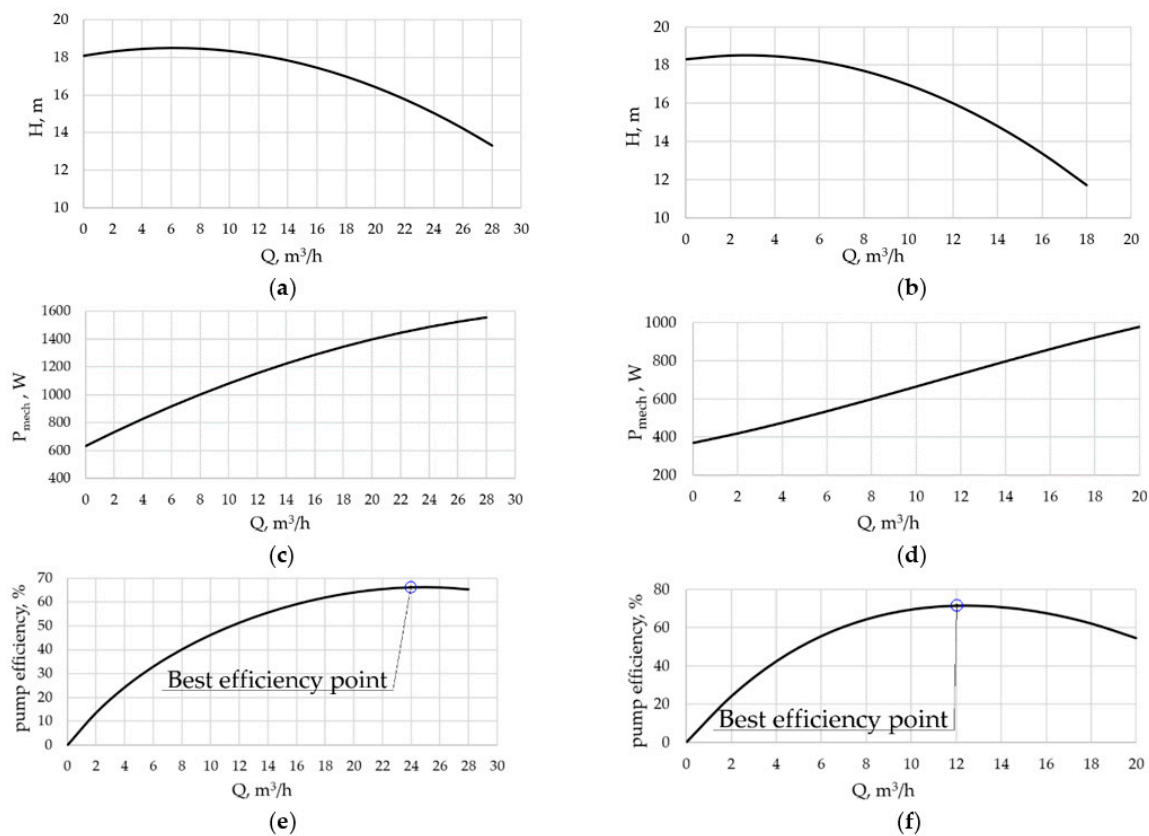


Figure 2. Pump characteristics [1] (a) model 1, Q - H curve; (b) model 2, Q - H curve; (c) model 1, mechanical power versus flowrate; (d) model 2, mechanical power versus flowrate; (e) model 1, efficiency versus flowrate; (f) model 2, efficiency versus flowrate.

3. Operating Point Calculation for Pumps

This section briefly describes the mathematical models of the examined pumping systems. In order to assess the characteristics of the operation mode of the pumps, the graphical analysis method is used. Figure 3a represents a single-pump system. Figure 3b represents a multi-pump system. Pumps P and $P1$ are coupled with induction motors M and $M1$, respectively. Frequency converters (FC) feed these motors. Pump $P2$ is coupled with induction motor $M2$. The throttle V is equipped with drive $M3$ (throttle control) and when the pumps operate simultaneously, it is regulated together with the electric drive $M1$. The rest of the valves shown in Figure 3 as well as non-return valves are used for protective purposes not for control.

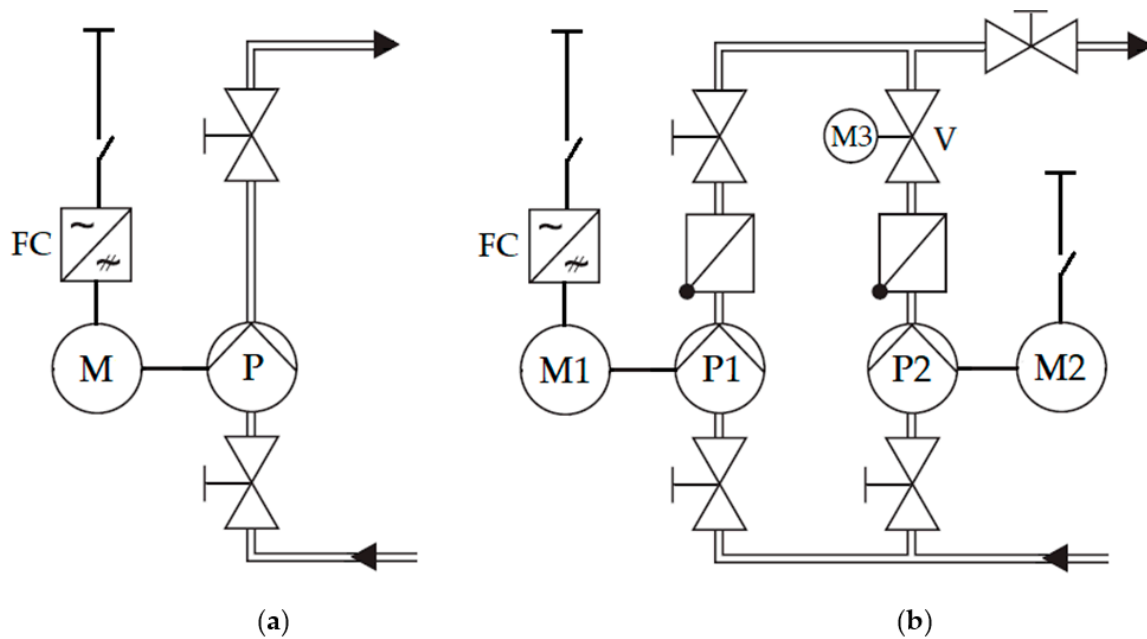


Figure 3. Pumping system structure: (a) single-pump, power 1500 W; (b) multi-pump, each of the pump has a nominal power of 750 W.

The values of Q and H of individual pumps are calculated according to their technical characteristics (Figure 2). During the development of a mathematical model for the pump system, polynomial interpolations of the technical characteristics of the pumps are used [8,23]. The mathematical model of a multi-pump system consisting of two similar pumps and a hydraulic load is described by the following equations [8,23]:

$$H_1 = a \cdot Q_1^2 + b \cdot Q_1 \cdot s_1 + c \cdot s_1^2 \quad (1)$$

$$H_2 = a \cdot Q_2^2 + b \cdot Q_2 \cdot s_2 + c \cdot s_2^2 \quad (2)$$

$$H_{req} = H_{st} + k \cdot Q_{req}^2 \quad (3)$$

where Q_1 and H_1 are the flowrate and the head of the variable speed controlled pump; Q_2 and H_2 are the flowrate and the head of the non-adjustable speed pump; $a = -0.02903$, $b = 0.15655$, and $c = 18.284$ are the coefficients of the interpolation polynomial obtained according to the Q - H characteristics of pump Calpeda—B—NM 32/12D at the rated rotational speed (Figure 2); s_1 and s_2 are the rotational speeds of the variable speed and non-adjustable speed pumps in relative units ($s_1 = n_1/n_{rate}$; $s_2 = n_2/n_{rate}$); n_1 and n_2 are the rotational speeds in absolute values; $n_{rate} = 2900$ rpm; Q_{req} and H_{req} are the required values of the water supply and hydraulic head (hydraulic loads); H_{st} and k are the static head and the hydraulic friction coefficient of the hydraulic system.

The flowrate of separate pumps Q_1 and Q_2 and the total flowrate of the pumping system Q_{req} are related according to Equation (4) [8]:

$$Q_{req} = Q_1 + Q_2 \quad (4)$$

The friction coefficient k is defined as:

$$k = \frac{H_{max} - H_{st}}{Q_{max}^2} \quad (5)$$

where $H_{max} = 16$ m, $Q_{max} = 24$ m³/h, $H_{st} = 0.5 \cdot H_{max}$ [25].

To calculate the variation of flow Q , head H , and power on the shaft P_{mech} at different rotational speeds, the affinity laws are applied [23]:

$$\frac{Q_{N1}}{Q_{N2}} = \frac{N_1}{N_2}; \frac{H_{N1}}{H_{N2}} = \left(\frac{N_1}{N_2}\right)^2; \frac{P_{mech n1}}{P_{mech n2}} = \left(\frac{N_1}{N_2}\right)^3, \tag{6}$$

where Q_{N1} , H_{N1} and P_{mechN1} are the flowrate, pump head, and power on the shaft at speed $N_1 < n_{rate}$; Q_{N2} , H_{N2} and P_{mech} are the flowrate, pump head, and power on the shaft at speed $N_2 = n_{rate}$.

During the operation of pumps in parallel without throttling the flow Q of pumps in the multi-pump system sums up (4) at the same hydraulic head value. Then, the intersection point of the resulting performance H - Q curve and system curve is obtained (Figure 4).

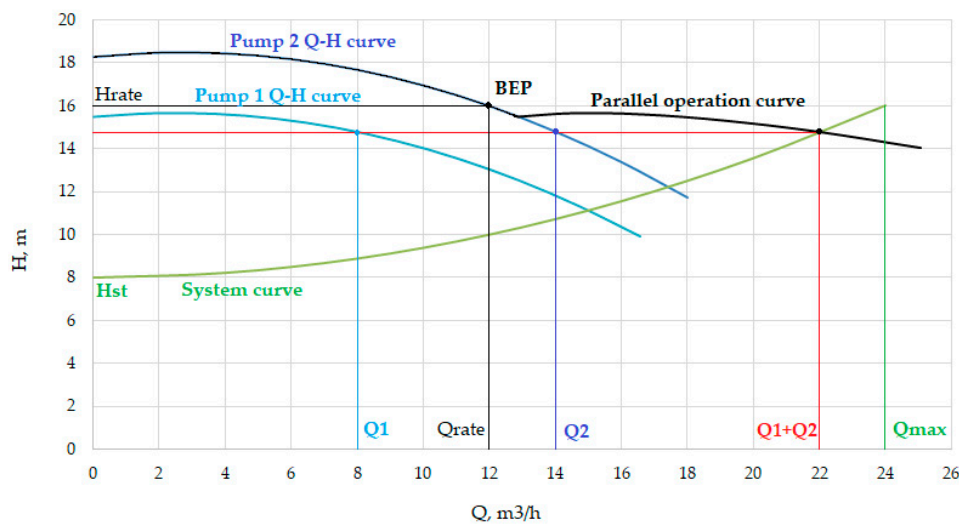


Figure 4. Calculation of the working point of the multi-pump system.

The algorithm for the graphical solution of the system of Equations (1)–(4) is explained below for parallel operation of two pumps, with one VSD. At a given value of the reference flowrate Q_{req} , Equation (3) determines the required value of the head H_{req} . Since the pumps operate at different rotational speeds, to achieve the same head $H_{pump1} = H_{pump2} = H_{req}$, the pump capacity in the absence of throttling should be different. The speed of the second pump with non-adjustable electric drive equals the rated speed (2900 rpm); therefore, $s_2 = 1$. According to Equations (2) and (4), the values of Q_2 and Q_1 are obtained as follows:

$$Q_2 = \frac{-b - \sqrt{b^2 - 4a(c - H_{req})}}{2a} \tag{7}$$

$$Q_1 = Q_{req} - Q_2 \tag{8}$$

To calculate the hydraulic head of the first pump, the affinity laws can be expressed in the following way (9):

$$\frac{H_1(n_1)}{H_1(n_{rate})} = s_1^2 \tag{9}$$

From Equation (1) taking into account affinity laws (6) and (9), the following equation is derived:

$$n_1 = n_{rate} \cdot \frac{-b \cdot Q_1 + \sqrt{(b \cdot Q_1)^2 - 4 \cdot c \cdot (a \cdot Q_1^2 - H_{req})}}{2c} \tag{10}$$

The greater the difference in rotational speed between the two pumps, the greater the difference between flowrate Q_1 and Q_2 . This condition leads to an overload of the non-adjustable pump and underload of the variable speed pump, which is not acceptable in terms of the energy efficiency point of view (at Q_{req} less 75% of Q_{max} , Q_1 becomes negative) [8]. This article considers the parallel operation of the pumps by ensuring equal flowrates of the two pumps with the help of throttling by using throttle $M3$ for the non-adjustable pump. Flowrates Q_1 and Q_2 are calculated according (11):

$$Q_1 = Q_2 = Q_{req}/2 \tag{11}$$

The control law (11) for parallel pumps is described in the literature and is widely used in practice [8]. In this case, the pump working points will be defined as the intersection points of the pump characteristics $Q_{req}/2$ (points 1 and 2, Figure 5). The performance curve of the first pump (VSD) should cross point 1 with coordinates $(Q_{req}/2; H_{req})$. The rotational speed of the first pump is determined by equation (9). The regulation throttle of the second pump (non-adjustable) is controlled to maintain $Q_2 = Q_{req}/2$.

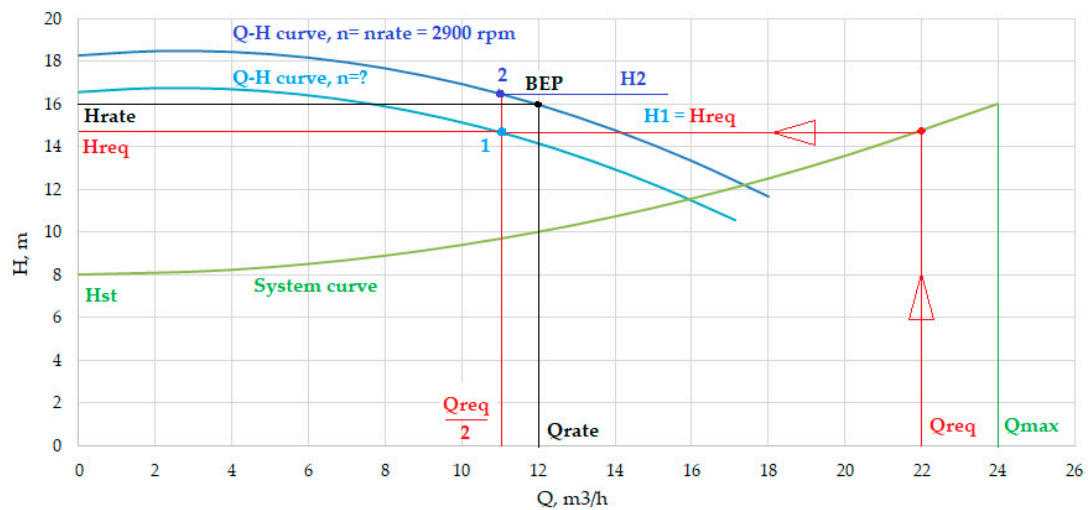


Figure 5. Pump working points in parallel operation.

4. Determination of Pump Characteristics and Mechanical Power during the Operation Cycle

To determine the performances of the above-mentioned pumping systems, first, mechanical powers P_{mech} are calculated, for ten different operation modes shown in Figure 1. Table 1 represents the calculated characteristics of the single pump system at ten different water flowrates, according to Figure 1. In the case of the single-pump system with one variable speed pump, the working points of the pumping system move along the system curve and are defined as intersection points of $Q-H$ pump characteristics at a certain rotation speed n and the hydraulic system curve.

Table 1. Operating cycle data for the single-pump system.

$Q_{req}, \%$	10	20	30	40	50	60	70	80	90	100
n, rpm	1918	1940	1991	2068.7	2181.4	2288	2424	2572	2731	2900
$Q_{req}, \text{m}^3/\text{h}$	2.4	4.8	7.2	9.6	12	14.4	16.8	19.2	21.6	24
H, m	8.07	8.28	8.63	9.13	9.89	10.53	12.39	12.51	13.7	15
P_{mech}, W	234	290	356	437	547	663	817	1002	12,223	14,856

The curve $Q-H$ and the mechanical power at a decrease in the pump rotational speed are calculated using affinity laws (6), (Figure 6).

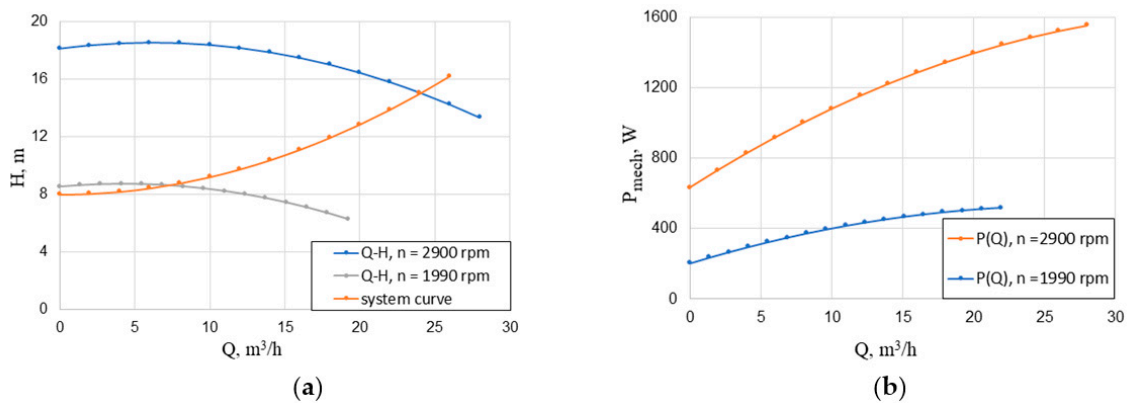


Figure 6. (a) Q-H characteristics of pump performance and system curve; (b) hydraulic power curves of the pump at different rotational speeds.

In the case of the joint operation, two similar pumps operate in parallel, and the total flowrate equals the sum of the flowrates of the individual pumps $Q = Q_1 + Q_2$. The first pump has an adjustable speed drive, and the rotation speed of the second pump is constant.

The range of the output flowrate can be divided into two parts:

- Water flowrate regulation in the range from 0 to 60% is achieved by speed variation of the variable speed pump. A non-adjustable pump in this range of flows is not switched on and is closed by a return valve to prevent water from flowing through it in the backward direction;
- Water flowrate regulation in the range from 60 to 100% is achieved by the operation of both pumps. Water is supplied by joint control of the rotational speed of the 1st pump according to the regulation law (10) and of throttling the 2nd pump. In a dynamic mode, this type of regulation can be achieved with the help of proportional-integral (PI) controllers.

In the case when the operation of the pumps in parallel is provided only by the rotation speed control of one of the pumps without throttling of a non-adjustable pump, the pump loading caused by flowrate will be different. The pump with a non-adjustable drive operating at nominal rotation speed will be overloaded and a variable speed drive will be underloaded. As the value of Q_{req} decreases, the load difference will increase. If the flow rate is such that for a given speed n_1 the head H_2 approximately equals or is greater than the shut-off head of the adjustable pump, then the flowrate of a variable speed pump will be close to zero (deadheading), or even negative (reverse flow). The reduction of the total flow of pumps operating in parallel by increasing the reverse flow of one of the pumps is identical to bypass-control. However, continuous operation of the pump in such modes is unacceptable due to low energy efficiency and can lead to deterioration of the pump equipment [2]. To avoid these operation modes, it is necessary to reduce the pressure in the pipeline connected to a non-adjustable pump with the help of throttling.

Based on the considerations given above, in the case of calculating the joint operation of two pumps in multi-pump system, the working points of the variable speed pump are determined in the same way as in the case of operation of one pump with a flow $Q_{req}/2$ according to Equations (1)–(3). The working point of the pump with a non-adjustable drive is determined by the intersection of its Q-H characteristics and vertical line $Q_{req}/2$. Table 2 represents the calculation results for these pumps operating in parallel for ten different modes of the cycle with the selected control method $Q_1 = Q_2$. Figure 7 also shows the calculated working points of these parallel pumps in terms of Q-H axes.

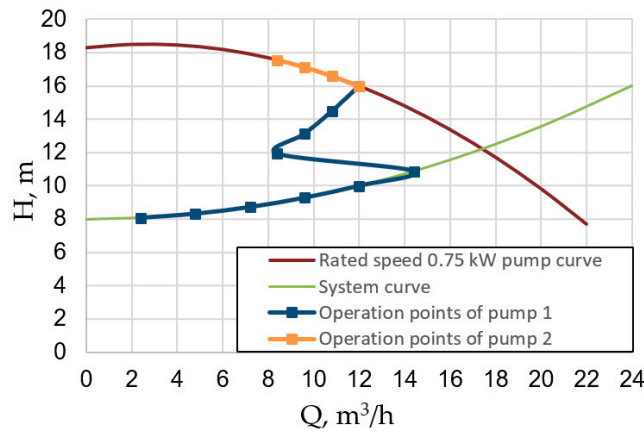


Figure 7. Working points of pumps operating in parallel.

Table 2. System cycle data for two pumps operating in parallel mode.

$Q_{req}, \%$	$Q_{req}, m^3/h$	$Q_1, m^3/h$	$Q_2, m^3/h$	H_1, m	H_2, m	P_{mech1}, W	P_{mech2}, W	$P_{mech} = P_{mech1} + P_{mech2}, W$	n_1, rpm	n_2, rpm
10	2.4	2.4	-	8.1	-	136	-	136	1918	-
20	4.8	4.8	-	8.3	-	181	-	181	1975	-
30	7.2	7.2	-	8.7	-	247	-	247	2081	-
40	9.6	9.6	-	9.3	-	338	-	338	2229	-
50	12	12	-	10.0	-	463	-	463	2409	-
60	14.4	14.4	-	10.9	-	628	-	628	2615	-
70	16.8	8.4	8.4	11.9	17.6	394	616	1010	2433	2900
80	19.2	9.6	9.6	13.1	17.1	486	654	1140	2579	2900
90	21.6	10.8	10.8	14.5	16.6	598	691	1289	2736	2900
100	24	12	12	16.0	16.0	730	729	1460	2901	2900

In Table 2 the following notation is used: P_{mech1} is the mechanical power of the variable speed pump; P_{mech2} is the mechanical power of the non-adjustable pump. As can be seen from Figure 7 and Table 2, when using the two pumps, the second parallel pump is used only at the required flow rate of 70% or more. Flow rates in the range of 0–60% can be provided by one of the lower power pumps. When both pumps are used, the equal distribution of the required flow rate $Q_1 = Q_2 = Q_{req}/2$ between them is adopted. As mentioned above, this control law provides minimum power consumption in this case. The head values of the two pumps are not equal to each other, $H_1 \neq H_2$, which is achieved by throttling the output of the second pump. The speed of the first pump n_1 is adjusted by the VSD. The rotational speed of the second pump powered directly from the mains is assumed to be constant, $n_2 = 2900$ rpm. The H_1 , H_2 , and n_1 values are calculated according to the method described in Section 3 (see Figure 5). The mechanical powers P_{mech1} and P_{mech2} are evaluated using the $P_{mech}(Q)$ dependence shown in Figure 2b. Figure 8 represents graphical dependencies of the total mechanical power of the two configurations of a pumping system on the water flowrate according to Tables 1 and 2. It can be seen that during the variation of the flowrate up to $Q_{req} = 14.4$ m³/h (60%), the multi-pump system demands less mechanical power. At higher Q_{req} , however, it requires more mechanical power than a system with a single pump.

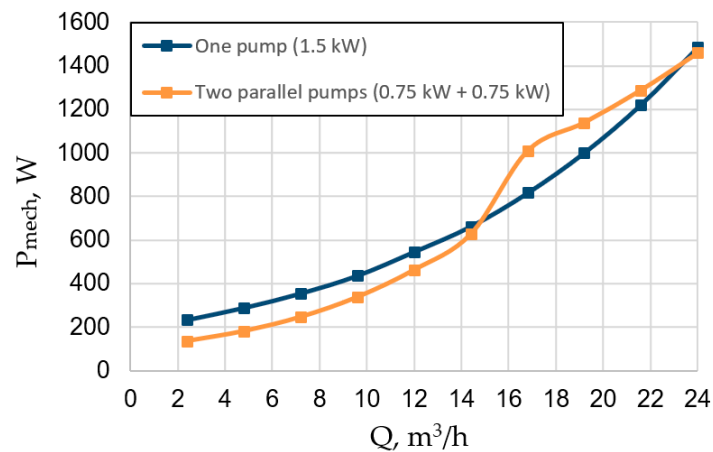


Figure 8. The mechanical power of the examined pumping units depending on the flowrate.

5. Assessment of Energy Consumption of the Two Considered Pump Systems

This section is focused on the electrical energy consumption calculation for the two configurations of the mentioned pump systems: single-pump (Figure 3a, Table 1) and multi-pump (Figure 3b, Table 2). In the current simulation, it was assumed that 2-pole induction motors with rated powers of 1500 W and 750 W are used in these pumping systems. These motors have the IE3 energy efficiency level. To determine the efficiency of motors and frequency converters at the operating points calculated in the previous section, the data for seven standard modes are used (according to IEC 60034-30-2) at a certain value of T and n (Table 3). Such data are used because the standard IEC 60034-30-2 [26] requires the motor manufacturers to declare the motor efficiency in these seven operating points. Some of the manufacturers provide such data in their catalogs [27]. The data in Table 3 related to the efficiency of the considered induction motors and frequency converters are obtained experimentally. These data were obtained from testing of M3AA90L2 and M3AA80B2 motors (IM-1.5 kW and IM-750 W, correspondingly, IE3-class, manufacturer ABB) [28] powered by a frequency converter with a rated power of 1.5 kW (model Optidrive P2, manufacturer Invertek Drives) [29]. This test was performed according to IEC 60034-2-3, Method 2-3-C: Input-output method (Figure 9).

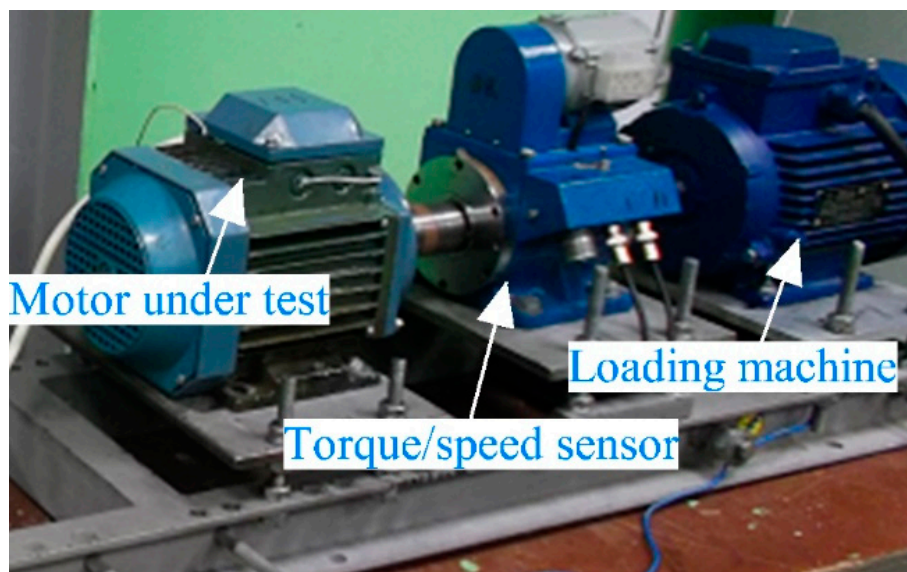


Figure 9. Test bench.

Table 3. Efficiency data for motors and FC at standard points, in accordance with IEC 60034-30-2.

Operation Point	1	2	3	4	5	6	7
$n, \%$	90	50	90	50	25	50	25
$T, \%$	100	100	50	50	100	25	25
η_{motor} IM-1.5 kW	0.853	0.728	0.865	0.819	0.533	0.822	0.772
η_{motor} IM-750 W	0.830	0.768	0.809	0.749	0.645	0.653	0.523
$\eta_{\text{conv.}}$ FC-1.5 kW	0.965	0.947	0.952	0.925	0.905	0.888	0.784
$\eta_{\text{conv.}}$ FC-750 W	0.937	0.906	0.898	0.849	0.857	0.771	0.686

The values of the efficiency of motors and frequency inverters in the considered operating points (Tables 1 and 2) found by the polynomial interpolation of the data in Table 3 [4,30] are shown in Table 4. The following notations are used in Table 4: η_{motor} is the motor efficiency of the single-pump system; η_{conv} is the frequency converter efficiency of the single-pump system; η_{motor1} is the motor efficiency of the multi-pump system for variable speed drive; η_{conv1} is the frequency converter efficiency of the multi-pump system for variable speed drive; η_{motor2} is the efficiency of non-adjustable motor in multi-pump system.

Table 4. The results of efficiency calculation for motors and frequency converters.

$Q_{\text{reqr}} \%$		10	20	30	40	50	60	70	80	90	100
$Q_{\text{reqr}} \text{ m}^3/\text{h}$		2.40	4.80	7.20	9.60	12.0	14.4	16.8	19.2	21.6	24.0
System with one pump (FC-IM)	η_{motor}	0.431	0.507	0.580	0.651	0.723	0.783	0.838	0.874	0.879	0.834
	$\eta_{\text{conv.}}$	0.939	0.944	0.950	0.955	0.960	0.963	0.964	0.961	0.957	0.952
Two parallel pumps (FC-IM1) + IM2	η_{motor1}	0.699	0.734	0.778	0.816	0.840	0.831	0.818	0.826	0.819	0.792
	η_{motor2}	-	-	-	-	-	-	0.796	0.797	0.796	0.792
	$\eta_{\text{conv.1}}$	0.431	0.507	0.580	0.651	0.723	0.783	0.838	0.874	0.879	0.834

With the help of the obtained results from tables (Tables 1, 2 and 4), we can calculate the electric power consumption from the network (P_1), daily electricity consumption (E_{day}), annual electricity consumption (E_{year}), total amount of annual electricity costs (C_{year}), and annual cost savings (S_{year}) for the multi-pump system with low-power pumps in comparison with the single-pump system:

$$P_1 = \frac{P_{\text{mech}}}{\eta_{\text{motor}} \cdot \eta_{\text{conv}}} \tag{12}$$

$$E_{\text{day}} = \frac{t_{\Sigma}}{1000} \cdot \sum_{i=1}^{10} \left(P_1(i) \cdot \frac{t_i}{t_{\Sigma}} \right) \tag{13}$$

$$E_{\text{year}} = E_{\text{day}} \cdot 365 \tag{14}$$

$$C_{\text{year}} = E_{\text{year}} \cdot GT \tag{15}$$

$$S_{\text{year}} = C_{\text{year2}} - C_{\text{year1}} \tag{16}$$

where P_{mech} , and η_{motor} are the mechanical power and efficiency of m -th electrical motor in the i -th operation mode; η_{conv} is the efficiency of m -th frequency converter in the i -th operation mode; t_{Σ} is the 24 h cycle time; t_i is the duration of the i -th operation mode; $GT = 0.2036 \text{ €/kWh}$ is the electrical energy costs in Germany in the second quarter of 2019 for 1 kW·h for industrial applications [31]; C_{year1} and C_{year2} are the total annual energy costs of the multi-pump system (two pumps) and single-pump (one pump) system configurations.

The results of the calculation according to Equations (12)–(16) are shown in Tables 5 and 6. Figure 10 shows the dependence of the electric power consumption by the pumping systems from the grid for the mentioned cases. The energy saving possibilities were calculated according to the data in Table 5 (Table 6). Thus, in the case of the multi-pump system (two parallel pumps), the energy

consumption is higher in comparison with a single-pump unit, in the rare operation modes when the two pumps operate together. However, significant energy savings can be achieved in operation modes when one of the pumps of the multi-pump system can provide the required flowrate. As a result, in the case of the multi-pump system (two parallel pumps), the energy consumption during the working cycle is reduced by 29.8% in comparison with the single-pump system.

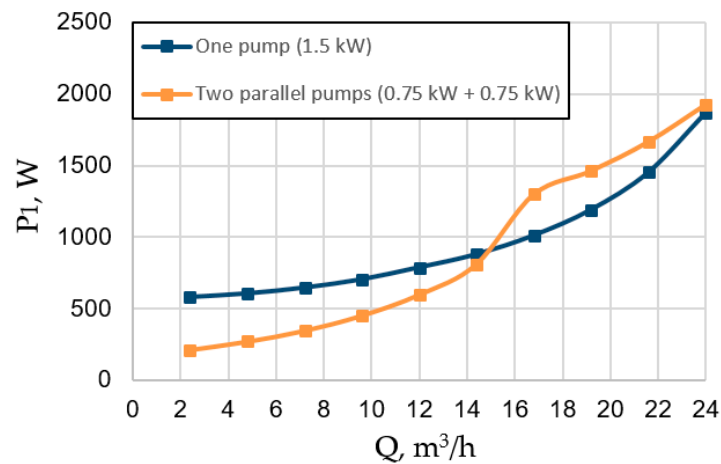


Figure 10. Electrical power consumption of the pumping systems depending on the flowrate.

Table 5. Electric power consumption of pumping systems for various flowrate modes.

$Q_{req}, \%$	10	20	30	40	50	60	70	80	90	100
$Q_{req}, m^3/h$	2.40	4.80	7.20	9.60	12.0	14.4	16.8	19.2	21.6	24.0
P_1, W Two parallel pumps	213	272	347	453	599	812	1300	1465	1668	1928
One pump	580	605	646	704	788	880	1012	1192	1454	1872

Table 6. Comparison of a system’s power consumption.

Pump System	E_{day}, kWh	E_{year}, kWh	$C_{year}, €$	$S_{year}, \%$	$S_{year}, €$
Two parallel pumps (FC-IM1) + IM2	12.37	4516	919	29.8	391.1
System with one pump (FC-IM)	17.63	6437	1310	-	-

6. Conclusions

The article provides a comprehensive comparison and analysis of energy consumption for the multi-pump system consisting of two pumps operating in parallel mode and the single-pump system:

- The single-pump system is equipped with a single variable speed drive. The multi-pump system is equipped with one variable speed drive that is fed by a frequency converter and a non-adjustable drive connected directly to a grid;
- The comparison of energy consumption for both pump system configurations shows that the usage of a multi-pump system supplied with two low-power pumps instead of a high-power pump in the single-pump system can lead to 29.8% energy savings;
- The energy savings are achieved due to the application of pumps and variable speed drives with a lower rated power and, therefore, with low losses in the operation modes in which the flowrate can be provided by one of the two pumps.
- Despite a rather low efficiency of the multi-pump system at high flowrates, the gain in the efficiency at the most frequent low flowrates results in an increase in the overall efficiency and energy saving.

- In future works, the optimization of the energy consumption of the considered configurations of multi-pump systems will be presented using mathematical optimization methods, considering the characteristics of motors and frequency converters.

Author Contributions: Conceptual approach, V.K. and V.P.; data curation L.G., and V.D.; software S.O. and V.K.; calculations and modeling, S.O, V.K., and V.P.; writing of original draft, L.G., S.O., V.D., V.K. and V.P.; visualization, L.G., S.O. and V.K.; review and editing, L.G., S.O., V.D., V.K. and V.P. All authors have read and agreed to the published version of the manuscript.

Funding: The work was partially supported by the Ministry of Science and Higher Education of the Russian Federation (through the basic part of the government mandate, Project No. FEUZ-2020-0060).

Acknowledgments: The authors thank the editors and reviewers for careful reading and constructive comments.

Conflicts of Interest: The authors declare no conflict of interest.

References

1. European Commission. *Study on Improving the Energy Efficiency of Pumps*; Standards Publishing: London, UK, 2001.
2. Nelik, L. *Centrifugal and Rotary Pumps. Fundamentals with Applications*; CRC Press: Boca Raton, FL, USA, 1999.
3. Goman, V.; Oshurbekov, S.; Kazakbaev, V.; Prakht, V.; Dmitrievskii, V. Energy Efficiency Analysis of Fixed-Speed Pump Drives with Various Types of Motors. *Appl. Sci.* **2019**, *9*, 5295. [[CrossRef](#)]
4. Kazakbaev, V.; Prakht, V.; Dmitrievskii, V.; Ibrahim, M.N.; Oshurbekov, S.; Sarapulov, S. Efficiency Analysis of Low Electric Power Drives Employing Induction and Synchronous Reluctance Motors in Pump Applications. *Energies* **2019**, *12*, 1144. [[CrossRef](#)]
5. Shankar, V.K.A.; Umashankar, S.; Paramasivam, S.; Hanigovszki, N. A comprehensive review on energy efficiency enhancement initiatives in centrifugal pumping system. *Appl. Energy* **2016**, *181*, 495–513. [[CrossRef](#)]
6. Viholainen, J. Energy-Efficient Control Strategies for Variable Speed Driven Parallel Pumping System Based on Pump Operation Point Monitoring with Frequency Converters. Ph.D Thesis, Lappeenranta University of Technology, Lappeenranta, Finland, 2014.
7. Ahonen, T. Monitoring of Centrifugal Pump Operation by a Frequency Converter. Ph.D. Thesis, Lappeenranta University of Technology, Lappeenranta, Finland, 2011.
8. Wu, P.; Lai, Z.; Wu, D.; Wang, L. Optimization Research of Parallel Pump System for Improving Energy Efficiency. *J. Water Resour. Plan. Manag.* **2015**, *141*, 04014094. [[CrossRef](#)]
9. Viholainen, J.; Tamminen, J.; Ahonen, T.; Ahola, J.; Vakkilainen, E.; Soukka, R. Energy-efficient control strategy for variable speed-driven parallel pumping systems. *Energy Effic.* **2012**, *6*, 495–509. [[CrossRef](#)]
10. Koor, M.; Vassiljev, A.; Koppel, T. Optimal Pump Count Prediction Algorithm for Identical Pumps Working in Parallel Mode. *Procedia Eng.* **2014**, *70*, 951–958. [[CrossRef](#)]
11. Wen, Y.; Zhang, X.; Wang, P. The Relationship Between the Maximum Efficiency and the Flow of Centrifugal Pumps in Parallel Operation. *J. Press. Vessel. Technol.* **2010**, *132*, 034501. [[CrossRef](#)]
12. Olszewski, P.; Arafeh, J. Parametric analysis of pumping station with parallel-configured centrifugal pumps towards self-learning applications. *Appl. Energy* **2018**, *231*, 1146–1158. [[CrossRef](#)]
13. Olszewski, P. Genetic optimization and experimental verification of complex parallel pumping station with centrifugal pumps. *Appl. Energy* **2016**, *178*, 527–539. [[CrossRef](#)]
14. Ahmed, A.; Moharam, B.; Rashad, E. Power Saving of Multi Pump-Motor Systems Using Variable Speed Drives. In Proceedings of the 2018 Twentieth International Middle East Power Systems Conference (MEPCON), Cairo, Egypt, 18–20 December 2018.
15. Pandey, S.; Singh, R.P.; Mahar, P.S. Optimal Pipe Sizing and Operation of Multistage Centrifugal Pumps for Water Supply. *J. Pipeline Syst. Eng. Pr.* **2020**, *11*, 04020007. [[CrossRef](#)]
16. Jia, M.; Zhang, J.; Xu, Y. Optimization Design of Industrial Water Supply Pump Station Considering the Influence of Atmospheric Temperature on Operation Cost. *IEEE Access* **2020**, *8*, 161702–161712. [[CrossRef](#)]
17. Luo, Y.; Xiong, Z.; Sun, H.; Guo, Y. Research on energy-saving operation control model of the multi-type configuration centrifugal pump system with single invert. *Adv. Mech. Eng.* **2017**, *9*, 1–10. [[CrossRef](#)]
18. Sike, H.; Xuejing, J.; Huifen, G. Optimization of the Number of Multiple Pumps Running Simultaneously in Open Cycle Cooling Water System in Power Plant. *Energy Procedia* **2012**, *17*, 1161–1168. [[CrossRef](#)]

19. Jepsen, K.L.; Hansen, L.; Mai, C.; Yang, Z. Power consumption optimization for multiple parallel centrifugal pumps. In Proceedings of the 2017 IEEE Conference on Control Technology and Applications (CCTA), Mauna Lani, HI, USA, 27–30 August 2017.
20. Saggewiss, G.; Kotwitz, R.; McIntosh, D. AFD synchronizing applications: Identifying potential methods and benefits. In Proceedings of the 2001 Petroleum and Chemical Industry Technical Conference (Cat. No.01CH37265), Toronto, ON, Canada, 26 September 2001; pp. 83–89. [[CrossRef](#)]
21. Automation Pump, Pump Genius. Product Description, WEG. Document Code: 50059602, Revision 04, January 2019. Available online: <https://static.weg.net/medias/downloadcenter/hb3/hda/WEG-pump-genius-50059602-brochure-en.pdf> (accessed on 1 December 2020).
22. Low Voltage AC Drives for Water, Wastewater & Irrigation Applications, FRENIC-AQUA, Product Description, Fuji Electric. Document Code: 24A1-E-0013, August 2012. Available online: https://www.fujielectric.com/products/ac_drives_lv/frenic-aqua/info/function.html (accessed on 1 December 2020).
23. Stoffel, B. *Assessing the Energy Efficiency of Pumps and Pump Units*, 1st ed.; Elsevier: Darmstadt, Germany, 2015.
24. Calpeda, N.M. *Close Coupled Centrifugal Pumps with Flanged Connections, Catalogue*; Calpeda S.p.A: Vicenza, Italy, 2018.
25. Europump. *Extended Product Approach for Pumps*; Europump: Brussels, Belgium, 2014.
26. *Rotating Electrical Machines—Part 2-3: Specific Test Methods for Determining Losses and Efficiency of Converter-Fed AC Induction Motors*; IEC 60034-2-3/Ed1; Standards Publishing: Geneva, Switzerland, 2013.
27. *The World's Most Efficient Magnet-less Pump Motor*; KSB SuPremE in IE5; KSB AG: Frankenthal, Germany, 2020.
28. Low Voltage Process Performance Motors according to EU MEPS, Catalog, ABB, Document Code: 9AKK105944 EN 11-2014, October 2014. Available online: [https://library.e.abb.com/public/23ff859eee0200c3c1257e1a002770a2/Catalog_Process_performance_acc_to_EU_MEPS_9AKK105944%20EN%2010_2014.low.pdf](https://library.e.abb.com/public/23ff859eee0200c3c1257e1a002770a2/Catalog_Process_performance_acc_to_EU_MEPS_9AKK105944%20EN%2010_2014.low.pdf?filename=Catalog_Process_performance_acc_to_EU_MEPS_9AKK105944%20EN%2010_2014.low.pdf) (accessed on 1 December 2020).
29. *Optidrive P2, AC Variable Speed Drive, 0.75 kW–250 kW / 1HP–350HP, 200–480 Volt 1 & 3 Phase*; Advanced User Guide, Revision 1.00; Invertek Drives Ltd.: Buttington, UK, 2012; Available online: <https://inverterdrive.com/file/Invertek-P2-Advanced-Guide> (accessed on 1 December 2020).
30. Safin, N.; Kazakbaev, V.; Prakht, V.; Dmitrievskii, V.; Sarapulov, S. Interpolation and analysis of the efficiency of a synchronous reluctance electric drive at various load points of a fan profile. In Proceedings of the 2018 25th International Workshop on Electric Drives: Optimization in Control of Electric Drives (IWED), Moscow, Russia, 31 January–2 February 2018.
31. Eurostat Data. *Eurostat Data for the Industrial Consumers in Germany*; Eurostat: Eurostat—European Statistics; European Commission: Luxembourg, 2019.

Publisher's Note: MDPI stays neutral with regard to jurisdictional claims in published maps and institutional affiliations.



© 2020 by the authors. Licensee MDPI, Basel, Switzerland. This article is an open access article distributed under the terms and conditions of the Creative Commons Attribution (CC BY) license (<http://creativecommons.org/licenses/by/4.0/>).